Workflow: Annotated pdf, CrossRef and tracked changes

PROOF COVER SHEET

Author(s): Manu Lopus
Article title: Elucidation of the anticancer potential and tubulin isotype-specific interactions of β-sitosterol
Article no: TBSD 1271749
Enclosures: 1) Query sheet
2) Article proofs

Dear Author,

1. Please check these proofs carefully. It is the responsibility of the corresponding author to check these and approve or amend them. A second proof is not normally provided. Taylor & Francis cannot be held responsible for uncorrected errors, even if introduced during the production process. Once your corrections have been added to the article, it will be considered ready for publication.

Please limit changes at this stage to the correction of errors. You should not make trivial changes, improve prose style, add new material, or delete existing material at this stage. You may be charged if your corrections are excessive (we would not expect corrections to exceed 30 changes).

For detailed guidance on how to check your proofs, please paste this address into a new browser window: http://journalauthors.tandf.co.uk/production/checkingproofs.asp

Your PDF proof file has been enabled so that you can comment on the proof directly using Adobe Acrobat. If you wish to do this, please save the file to your hard disk first. For further information on marking corrections using Acrobat, please paste this address into a new browser window: http://journalauthors.tandf.co.uk/production/acrobat.asp

2. Please review the table of contributors below and confirm that the first and last names are structured correctly and that the authors are listed in the correct order of contribution. This check is to ensure that your name will appear correctly online and when the article is indexed.

Sequence	Prefix	Given name(s)	Surname	Suffix
1		Madhura	Pradhan	
2		Charu	Suri	
3		Sinjan	Choudhary	
4		Pradeep Kumar	Naik	
5		Manu	Lopus	

Queries are marked in the margins of the proofs, and you can also click the hyperlinks below.
Content changes made during copy-editing are shown as tracked changes. Inserted text is in red font and revisions have a red indicator. Changes can also be viewed using the list comments function. To correct the proofs, you should insert or delete text following the instructions below, but **do not add comments to the existing tracked changes**.

AUTHOR QUERIES

General points:

1. **Permissions:** You have warranted that you have secured the necessary written permission from the appropriate copyright owner for the reproduction of any text, illustration, or other material in your article. Please see http://journalauthors.tandf.co.uk/permissions/usingThirdPartyMaterial.asp.
2. **Third-party content:** If there is third-party content in your article, please check that the rightsholder details for re-use are shown correctly.
3. **Affiliation:** The corresponding author is responsible for ensuring that address and email details are correct for all the co-authors. Affiliations given in the article should be the affiliation at the time the research was conducted. Please see http://journalauthors.tandf.co.uk/preparation/writing.asp.
4. **Funding:** Was your research for this article funded by a funding agency? If so, please insert 'This work was supported by <insert the name of the funding agency in full>', followed by the grant number in square brackets '[grant number xxxx]'.
5. **Supplemental data and underlying research materials:** Do you wish to include the location of the underlying research materials (e.g. data, samples or models) for your article? If so, please insert this sentence before the reference section: 'The underlying research materials for this article can be accessed at <full link>/ description of location [author to complete]'. If your article includes supplemental data, the link will also be provided in this paragraph. See <http://journalauthors.tandf.co.uk/preparation/multimedia.asp> for further explanation of supplemental data and underlying research materials.
6. The **CrossRef database** (www.crossref.org/) has been used to validate the references. Changes resulting from mismatches are tracked in red font.

AQ1	Please provide missing department for affiliation 'b'.
AQ2	The disclosure statement has been inserted. Please correct if this is inaccurate.
AQ3	Please note that the Funding section has been created from information provided through CATS and also check the grant number. Please correct if this is inaccurate.
AQ4	The CrossRef database (www.crossref.org/) has been used to validate the references. Mismatches between the original manuscript and CrossRef are tracked in red font. Please provide a revision if the change is incorrect. Do not comment on correct changes.
AQ5	Please check the author name "J. V. Postma" given for reference "Berendsen et al., 1984" and resupply if inaccurate.
AQ6	The reference 'Case et al. (2005)' is listed in the references list but is not cited in the text. Please either cite the reference or remove it from the references list.
AQ7	Please provide missing last page number for the "Jin et al., 2016" references list entry.

How to make corrections to your proofs using Adobe Acrobat/Reader

Taylor & Francis offers you a choice of options to help you make corrections to your proofs. Your PDF proof file has been enabled so that you can mark up the proof directly using Adobe Acrobat/Reader. This is the simplest and best way for you to ensure that your corrections will be incorporated. If you wish to do this, please follow these instructions:

1. Save the file to your hard disk.

2. Check which version of Adobe Acrobat/Reader you have on your computer. You can do this by clicking on the "Help" tab, and then "About".

   If Adobe Reader is not installed, you can get the latest version free from http://get.adobe.com/reader/.

3. If you have Adobe Acrobat/Reader 10 or a later version, click on the "Comment" link at the right-hand side to view the Comments pane.

4. You can then select any text and mark it up for deletion or replacement, or insert new text as needed. Please note that these will clearly be displayed in the Comments pane and secondary annotation is not needed to draw attention to your corrections. If you need to include new sections of text, it is also possible to add a comment to the proofs. To do this, use the Sticky Note tool in the task bar. Please also see our FAQs here: http://journalauthors.tandf.co.uk/production/index.asp.

5. Make sure that you save the file when you close the document before uploading it to CATS using the "Upload File" button on the online correction form. If you have more than one file, please zip them together and then upload the zip file.

   If you prefer, you can make your corrections using the CATS online correction form.

Troubleshooting

Acrobat help: http://helpx.adobe.com/acrobat.html
Reader help: http://helpx.adobe.com/reader.html

Please note that full user guides for earlier versions of these programs are available from the Adobe Help pages by clicking on the link "Previous versions" under the "Help and tutorials" heading from the relevant link above. Commenting functionality is available from Adobe Reader 8.0 onwards and from Adobe Acrobat 7.0 onwards.

Firefox users: Firefox's inbuilt PDF Viewer is set to the default; please see the following for instructions on how to use this and download the PDF to your hard drive: http://support.mozilla.org/en-US/kb/view-pdf-files-firefox-without-downloading-them#w_using-a-pdf-reader-plugin

TBSD 1271749
23 December 2016
Initial
CE: SL QA: PS

Journal of Biomolecular Structure and Dynamics, 2016
http://dx.doi.org/10.1080/07391102.2016.1271749

Elucidation of the anticancer potential and tubulin isotype-specific interactions of β-sitosterol

Madhura Pradhan[a,†], Charu Suri[b,†,§], Sinjan Choudhary[a], Pradeep Kumar Naik[c] and Manu Lopus[a*]

[a]*Experimental Cancer Therapeutics and Chemical Biology, UM-DAE Centre for Excellence in Basic Sciences, University of Mumbai Kalina Campus, Santacruz (E), Mumbai 400098, India;* [b]*Jaypee University of Information Technology, Waknaghat, Solan 173234, Himachal Pradesh, India;* [c]*School of Life Sciences, Sambalpur University, Jyoti Vihar, Sambalpur 768019, Odisha, India*

Communicated by Ramaswamy H. Sarma

(*Received 5 August 2016; accepted 2 December 2016*)

Beta-sitosterol (β-SITO), a phytosterol present in many edible vegetables, has been reported to possess antineoplastic properties and cancer treatment potential. We have shown previously that it binds at a unique site (the 'SITO-site') compared to the colchicine binding site at the interface of α- and β-tubulin. In this study, we investigated the anticancer efficacy of β-SITO against invasive breast carcinoma using MCF-7 cells. Since 'isotypes' of β-tubulin show tissue-specific expression and many are associated with cancer drug resistance, using computer-assisted docking and atomistic molecular dynamic simulations, we also examined its binding interactions to all known isotypes of β-tubulin in αβ-tubulin dimer. β-SITO inhibited MCF-7 cell viability by up to 50%, compared to vehicle-treated control cells. Indicating its antimetastatic potential, the phytosterol strongly inhibited cell migration. Immunofluorescence imaging of β-SITO-treated MCF-7 cells exhibited disruption of the microtubules and chromosome organization. Far-UV circular dichroism spectra indicated loss of helical stability in tubulin when bound to β-SITO. Docking and MD simulation studies, combined with MM-PBSA and MM-GBSA calculations revealed that β-SITO preferentially binds with specific β-tubulin isotypes (β_{II} and β_{III}) in the αβ-tubulin dimer. Both these β-tubulin isotypes have been implicated in drug resistance against tubulin-targeted chemotherapeutics. Our data show the tubulin-targeted anticancer potential of β-SITO, and its potential clinical utility against β_{II} and β_{III} isotype-overexpressing neoplasms.

Keywords: β-sitosterol; molecular dynamic simulations; breast cancer; microtubule; β-tubulin isotypes

Introduction

Tubulin, the building block of cylindrical, dynamic polymers called microtubules, is a guanine nucleotide-binding heterodimer with one alpha subunit and one beta subunit. A plethora of proteins, including G-proteins and EB1 (Dave et al., 2011; Lopus et al., 2012), have been known to regulate the assembly dynamics of microtubules. In addition, the β subunit of tubulin has eight 'isotypes', classified based on their C-terminal amino acid composition (Janke, 2014). These isotypes, which are mostly tissue-specific in expression, are known to slightly alter the assembly properties of microtubules, and many of them have been associated with resistance against tubulin-targeted drugs that work by perturbing the natural assembly dynamics of microtubules and thereby inhibiting cell proliferation (Dumontet & Jordan, 2010).

Dietary phytosterols are known to play a major role in inhibiting carcinogenesis and impeding tumor progression (Awad, Downie, Fink, & Kim, 2000; Awad & Fink, 2000; Jiménez-Escrig, Santos-Hidalgo, & Saura-Calixto, 2006). In our ongoing efforts to identify potential natural product drug molecules, we examined the anticancer mechanism of a phytosterol called beta sitosterol (β-SITO), a major constituent in several edible plant products, including pomegranate, peanut, almond, and avocado (Jiménez-Escrig et al., 2006). Anticancer potential of β-SITO against chemically induced cancers has been known for the past three decades (Awad & Fink, 2000). For example, Awad et al., found that it can effectively retard growth and metastasis of aggressively invasive breast tumors (Awad et al., 2000). Specifically, in rats, which were fed .2% β-SITO in the diet for about 7 months, there was a significant reduction (~40%) in the number of the animals that developed the chemically induced tumor (Awad et al., 2000). β-SITO has also been known for its efficacy against prostate, breast, and colon cancers (Awad, Chen, Fink, & Hennessey, 1996; von Holtz, Fink, & Awad, 1998; Vundru, Kale, & Singh, 2013). Our preliminary biochemical studies identified a unique binding site for this phytosterol on tubulin (Mahaddalkar, Suri, Naik, & Lopus, 2015).

*Corresponding author. Email: manu.lopus@cbs.ac.in
†These authors contributed equally to this work.
§Present address: Drug Discovery Research Centre Translational Health Science and Technology Institute, 3rd Milestone, Pali, Haryana 121004, India.

In this study, after examining the anticancer potential of β-SITO against breast cancer using cell model studies, and investigating its effect on the helical integrity of tubulin, we performed molecular docking and MD simulations to characterize its binding interactions with known isotypes of β-tubulin in αβ tubulin dimers to understand the fine details of its molecular mechanism of action and potential therapeutic implications.

Materials and methods

Materials

Chemicals, unless otherwise noted, were purchased from Sigma (St. Louis, MO). All reagents were of analytical grade. β-SITO was dissolved in dimethyl formamide (DMF) after purging the latter with argon.

Cell culture

Human breast adenocarcinoma cells (MCF-7) were from American Type Culture Collection (ATCC, Manassas, VA, USA). The cells were cultured in Dulbecco's Modified Eagles Medium (DMEM; Invitrogen, Carlsbad, CA) supplemented with 10% heat-inactivated fetal bovine serum (FBS, Invitrogen), 1% penicillin/streptomycin and 2 mM glutamine (Invitrogen), and were maintained at 5% CO_2 and 37 °C. Cells were passaged when plates were 70–80% confluent. The cells were determined to be free from mycoplasma as indicated by Hoechst 33342 staining (Life Technologies) and by MycoAlert Mycoplasma detection (Lonza, Basel, Switzerland).

Effects of β-SITO on MCF-7 cell viability

MCF-7 cells (5×10^4/mL) were plated in 96-well plates pre-coated with 10 µg/mL poly-L-lysine (Sigma, St. Louis, MO), and grown in DMEM containing 10% FBS. After 24 h of incubation, the cells were treated with different concentrations of β-SITO (0–30 µM) for 48 h, and the cell viability was assessed using 3-(45-dimethylthiazol-2-yl)-25-diphenyltetrazolium bromide assay (MTT assay). After the predefined time period, 10 µl MTT reagent (Sigma) at 5 mg/mL was added to each well and the wells incubated for 4 h at 37 °C; the resultant formazan crystals were dissolved in SDS-HCl (10% SDS in .01 N HCl). The readings were taken at 560 nm in a Tecan multimode reader (TECAN, Maennedorf, Switzerland). Nocodazole (10 µM) was used as the positive control.

Wound-healing assay

For scratch-wound assay to assess the effect of β-SITO on the breast cancer cell migration, the cells (7.5×10^4/mL) were seeded in poly-L-lysine-coated 12-well plates. Upon 90% confluency, the cell layer was 'wounded' by scratching the growth surface with a sterile pipette tip. The surface was then washed with 1 × PBS, photographed, and incubated in the absence or presence of β-SITO (20 µM), or nocodazole (1 µM), for 24 h. After the specified time point, matched-pair wound regions were photographed using a Nikon eclipse TS100 microscope (10 × magnification, N.A. = .25; Nikon, Tokyo, Japan). For each experiment, nine individual cell fields were recorded. The experiment was repeated twice.

Immunofluorescence microscopy of microtubules and DNA

MCF-7 cells were seeded at a density of 7.5×10^4 cells/mL on poly-L-lysine-coated coverslips. After incubation with the vehicle (.2% DMF), 20 µM β-SITO, 5 nM Taxol, or 1nM vinblastine for 24 h, the cells were washed twice in 1 × PBS, fixed with 3.7% paraformaldehyde at 37 °C for 20 min, and permeabilized with chilled methanol for 10 min at −20 °C. The cells were then washed with 1 × PBS, and the non-specific binding sites blocked with 5% horse serum in 1 × PBS. For staining the microtubules, the cells were incubated with anti α-tubulin antibodies (Sigma) for 1 h at 30 °C (1:300 dilution), and then with Alexa-568-conjugated antimouse IgG (Molecular Probes, Eugene, OR) for 1 h at 30 °C. The vehicle-treated cells were processed simultaneously. The coverslips were then mounted onto glass slides using Prolong Gold with 4',6-diamidino-2-phenylindole (DAPI; Molecular Probes), and imaged on a Nikon eclipse TE1000-U microscope (Nikon, Tokyo, Japan).

Conformational states of tubulin

We used a JASCO-810 circular dichroism spectrophotometer (JASCO, Tokyo, Japan) for obtaining Far-UV CD spectra. The instrument was thoroughly purged with nitrogen before starting the experiments. Tubulin (5 µM; purified from goat brain as described earlier, (Mahaddalkar et al., 2015) was incubated without or with 20 µM β-SITO in 25 mM Pipes buffer (pH 6.8) for 45 min at 35 °C. Then, CD spectra were taken in the range of 200–260 nm using a .2-cm path-length, quartz cuvette. For obtaining molar ellipticity from observed ellipticity, the following equation was used: $[\theta] = 100 \times (\theta/c \times l)$, where c is the concentration of the protein in mol/dm^3 and l is the path length of the cuvette in centimeters (Mahaddalkar et al., 2016). For each spectrum, the baseline correction was performed and the spectra were taken as an average of three accumulations with a scan rate of 100 nm/min). The experiment was repeated twice.

Computational docking of β-SITO to β-tubulin isotypes

Previously homology-modeled structures of αβ-heterodimer comprised α-tubulin and different isotypes of β-tubulin

(Santoshi & Naik, 2014) were used to investigate the binding affinity of β-SITO. Briefly, representative sequences of eight human β-tubulin isotypes [β_I (gi:18088719), β_{II} (gi:29788768), β_{III} (gi: 1297274), β_{IV} (gi: 135470), β_V (gi:14201536), β_{VI} (gi: 62903515), β_{VII} (gi:1857526) and β_{VIII} (gi:42558279)] from the NCBI database were used to build the structure of tubulin heterodimers. These sequences were aligned and compared using a multiple sequence alignment program. The sequences were observed to have mismatches at different positions with an identity score ranging from 77 to 94%. In particular, the mismatches were mostly concentrated in the region of residues 160–370 that constitutes the interface region between α- and β-tubulin (Supplementary Figure S1).

The αβ-tubulin dimers comprised α-tubulin and isotypes specific β-tubulin were homology modeled to retain the cofactors like GTP, GDP and Mg^{2+} at their respective sites as present in the template structure (PDB ID-1SA0), using Prime (Schrodinger Inc.). These tubulin dimers were then refined using protein minimization using Macromodel (Schrodinger, version 9.9) and OPLS force field with PRCG algorithm with an energy gradient of .001 kcal/mol. Molecular structure of β-SITO (Figure 1(A)) was built using Maestro (Schrodinger) followed by energy optimization using Macromodel (Schrodinger, version 9.9). Furthermore, it is geometrically optimized using Jaguar (version 7.7, Schrodinger) and using hybrid density functional theory with Becke's three-parameter exchange potential and the Lee–Yang–Parr correlation functional (B3LYP) with basis set 3-21G* (Becke, 1993; Binkley, Pople, & Hehre, 1980). After ensuring that the tubulin heterodimer and β-SITO are in correct form, molecular docking of the optimized ligand onto the tubulin dimer was carried out using Glide (version 4.5, Schrodinger, LLC). We have shown previously that the binding site of β-SITO on tubulin is unique compared to colchicine binding site based on competition binding assay between colchicine and β-SITO (Mahaddalkar et al., 2015). Further, blind docking experiment and MD simulation of the tubulin (PDB ID 1SA0)-β SITO complex revealed the amino acid composition of the β-SITO binding site. It consists of nine amino acids (five from β tubulin and four from α tubulin; Ala 99, Arg104,Trp 406, Gly 409, Ile 162, Val 254, Pro 260, Arg 261, Leu 262) which are unique and were not involved in the well-characterized colchicine binding site. Further, to enumerate the possible binding of β-SITO with isotypes specific β-tubulin in αβ-tubulin dimers, we adopted a blind docking approach, in which all the possible binding sites of tubulin dimer were predicted using SiteMap (version 2.4, Schrodinger) and were used for the molecular docking of β-SITO. The Glide grid receptor generation program with van der Waals scaling of .4 Å was employed for generating the receptor-grid file. A grid box size of 10 Å each for the

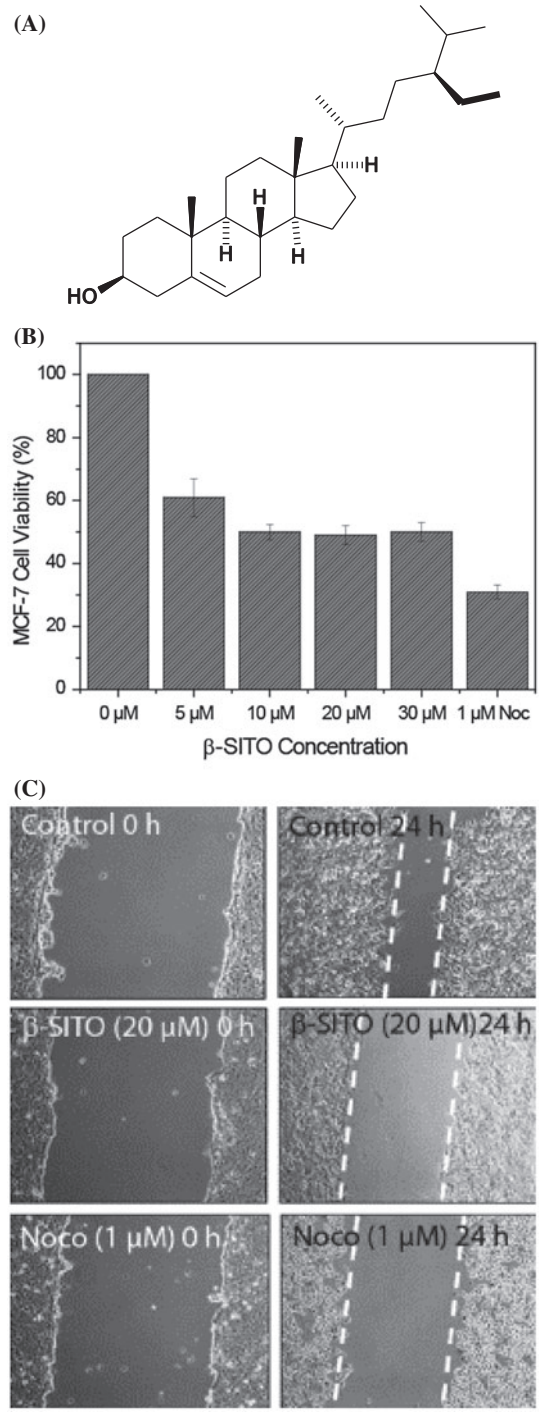

Figure 1. Beta-sitosterol (β-SITO) and its effects on MCF-7 breast cancer cells. (A) Structure of β-SITO. (B) Inhibition of MCF-7 viability by β-SITO. The cells were plated in 96-well plates and treated with different concentrations of β-SITO (0–30 μM) for 48 h, and the cell viability was assessed using an MTT assay, as described in Materials and Methods. Three independent experiments were performed (C). Inhibition of cell migration by β-SITO. The cells were seeded in poly-L-lysine-coated 12-well plates. Upon 90% confluency, the cell layer was wounded by scratching the growth surface with a pipette tip and the wound healing assay was performed as described in Materials and Methods. For each experiment, nine individual cell fields were recorded.

bounding and enclosing boxes was created at the centroid of the speculated binding sites. Beta-SITO was first docked using the Glide standard precision method and was further refined with Glide extra precision algorithm. The binding site having better docking score with β-SITO was selected as the putative binding site. Single best conformation for each β-SITO–tubulin complex was selected for further molecular modeling calculations.

Molecular dynamic simulation of β-SITO-β tubulin isotypes interactions

MD simulations were carried on all complexes obtained from the molecular docking of β-SITO with isotype specific β-tubulin in the αβ-tubulin dimers. The parameters and topology for β-SITO were generated using antechamber program implemented in Amber tools 1.5, using AM1-bond charge correction model to calculate the atomic point charges. The parameters for each tubulin isotype were generated using FF99SB, and forcefield parameters for Mg^{2+} ions, GTP and GDP were obtained from Bryce database (http://research.bmh.manchester.ac.uk/bryce/amber#cof) (Allnér, Nilsson, & Villa, 2012; Meagher, Redman, & Carlson, 2003). The topologies and coordinate files for all the complexes were generated using LEaP module in Ambertools 1.5. For all the eight complexes, missing hydrogens were assigned and subseqeuntly neutralized using sodium ions. Solvation of the complexes was accomplished using TIP3P water model in a truncated octahedron with a minimum distance of 15 Å between the wall of the box and the closest atom of the complex (Jorgensen, Chandrasekhar, Madura, Impey, & Klein, 1983). In order to relax the molecular systems and to remove bad contacts, for initial system preparation, all complexes comprising β-tubulin isotype and β-SITO were minimized three times, using 2 fs time step for 2000 steps each. We have used a combination of both steepest decent and conjugate gradient algorithm for the minimization. All the complexes were minimized for first 1000 steps using steepest decent method followed by conjugate gradient method for remaining 1000 steps. First and second rounds of minimizations imposed a positional restraint of 10 and 2 $kcal^{-1}Å^{-2}$, respectively, on tubulin to relax water molecules. The temperature of the molecular systems was progressively increased from 0 to 300 K; subsequent equilibration was performed for 500 ps at 300 K (pressure, 1 atm). After verifying stability of all thermodynamic properties, the complexes were simulated for 25 ns (2 fs time step) using PMEMD module in Amber 11 (Case et al., 2010) in isothermal-isobaric (NPT) ensemble. The electrostatic interactions were calculated using Particle Mesh Ewald (Darden, York, & Pedersen, 1993; Essmann et al., 1995) method and the bonds were constrained using Shake algorithm (Berendsen, Postma, van Gunsteren, DiNola, & Haak, 1984). The non-bonded cut-off distance was kept at 10 Å. The temperature was regulated using Langevin thermostat. Co-ordinates were written to the trajectory file at every 10 ps. A total of 25,000 frames was obtained after 25 ns simulation. All trajectories were analyzed using PTRAJ program implemented in Ambertools (Pearlman et al., 1995).

Calculation of binding free energy

Free energy binding of β-SITO to each isotype-specific β-tubulin in αβ-tubulin dimers was then calculated using MM-PBSA and MM-GBSA methods (Kollman et al., 2000; Massova & Kollman, 2000) implemented in Amber 11. Free energy binding and the energy components were calculated as the ensemble average of the binding free energy of a total of 500 snapshots, extracted every 10 ps from the last 5 ns of the MD simulation trajectory as follows:

$$\Delta G_{\text{bind}} = \Delta G_{\text{complex}} - [\Delta G_{\text{Rec}} + \Delta G_{\text{lig}}]$$

$$G = E_{\text{gas}} + G_{\text{sol}} - TS$$

$$E_{\text{gas}} = E_{\text{int}} + E_{\text{ele}} + E_{\text{vdw}}$$

$$G_{\text{sol}} = G_{\text{PB(GB)}} + G_{\text{sol-np}}$$

$$G_{\text{sol-np}} = \gamma_{\text{SAS}}$$

where G is Gibbs free energy, E_{gas} is the gas phase energy calculated as the sum of internal energy (E_{int}), energy generated as a result of the electrostatic interaction (E_{ele}), and the van der Waals interaction (E_{vdw}). G_{sol} is the solvation free energy calculated as the sum of polar ($G_{\text{PB(GB)}}$) and nonpolar contributions ($G_{\text{sol-np}}$). Polar interaction contribution ($G_{\text{PB(GB)}}$) was calculated as the summation of electrostatic contribution (E_{ele}) and polar solvation contribution ($G_{\text{PB(GB)}}$). The nonpolar solvation contribution ($G_{\text{sol-np}}$) is approximated as linearly dependent on the solvent accessible surface area (SAS) and γ is the surface tension constant that was set to .0072 kcal mol^{-1} $Å^{-2}$ (Sitkoff, Sharp, & Honig, 1994). The energy contribution for all amino acids in β-isotypes specific tubulin heterodimers was calculated to identify those residues of β-tubulin which show strong interaction with β-SITO.

Results

β-SITO inhibited viability and migration of MCF-7 cells

We first examined the potential of β-SITO (Figure 1(A)) to inhibit breast cancer cell viability using MCF-7 cells. β-SITO reduced the cell viability by 40% at a concentration of 5 μM and twice this concentration reduced the viability by 50% (Figure 1(B)). Interestingly, the

inhibition did not show any further downward trend, even after tripling the drug concentration (from 10 to 30 μM), indicating that β-SITO can inhibit cell viability without being extremely cytotoxic. The concentration of the drug could not be increased further due to precipitation. Wound-healing assay indicated strong inhibition of cell migration by β-SITO (20 μM). Specifically, compared to vehicle-treated control, β-SITO (20 μM) showed inhibition of cell migration similar to nocodazole, indicating the anti-invasive and anti-metastatic potential of the phytosterol against breast cancer cells (Figure 1(C)). However, to substantiate this conjecture, *in vivo* studies using metastatic tumor models are required.

Immunofluorescence microscopy of microtubules and DNA

For visualizing the effect of β-SITO on cellular microtubules, microtubules in MCF-7 cells grown in the absence and presence of β-SITO (20 μM) were observed using immunofluorescence microscopy. β-SITO exerted considerable damage amounting to the visible disruption of the spindle microtubules and resulted in chromosomal noncongression (Figure 2). Specifically, when probed with DAPI, the packing pattern of the genome appeared to be puffed up due to the disruption of the structural integrity of the spindle (Figure 2).

Perturbation of tubulin secondary structure by β-SITO

After ascertaining its effects on cellular microtubules, we asked whether β-SITO-induced disruption of microtubules involved loss of structural integrity of tubulin. We therefore tested the effect of the phytosterol on the helical content of tubulin using a far-UV circular dichroism. As illustrated in Figure 3, compared to control, β-SITO-treated tubulin showed alteration in its secondary structure, as evidenced by a reduction in the negative band, indicating that β-SITO does bind to tubulin and induces loss of helical stability of the protein.

Binding interactions of β-SITO with β-tubulin isotypes

After confirming β-SITO's ability to inhibit cell viability by disrupting microtubule network integrity through structural alterations in tubulin, we investigated the relative binding affinities of the compound to all known isotypes of β-tubulin (β_I to β_{VIII}; (Santoshi & Naik, 2014)) in αβ-tubulin dimer by a combination of molecular docking, MD simulation, and MM-GBSA/MM-PBSA calculations. Based on molecular docking, it was found that β-SITO binds well with different isotypes of tubulin. However, it showed a different docking score, docking energy, and H-bond energy with respect to different β tubulin isotypes in αβ-tubulin dimer (Supplementary Table 1). Based on docking energy, the phytosterol binds with high affinity to $\alpha\beta_{VI}$, (−37.919 kcal/mol) followed

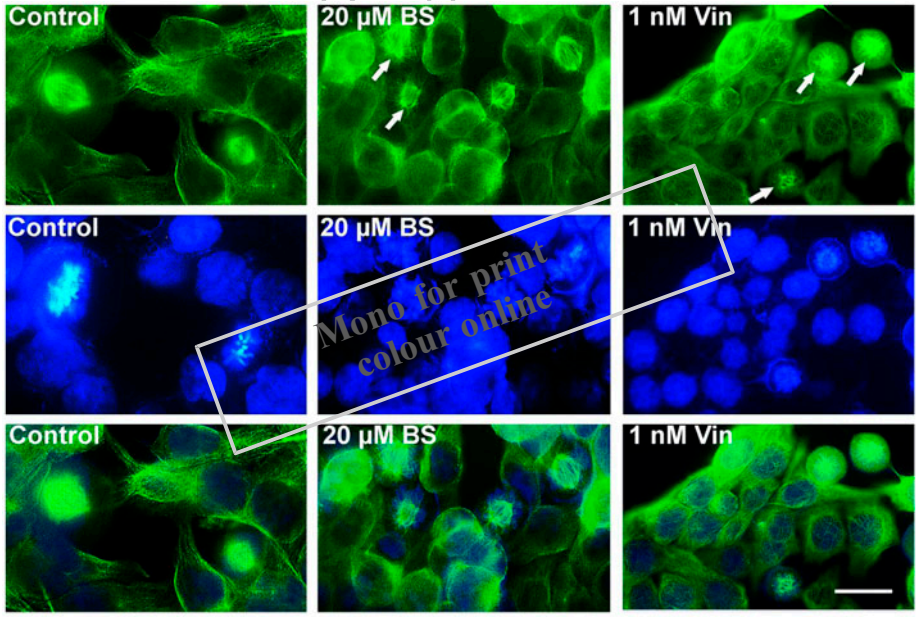

Figure 2. Disruption of cellular microtubules by β-SITO. The cells, treated with 20 μM β-SITO for 24 h were incubated with anti α-tubulin antibodies and Alexa-568-conjugated secondary antibodies to localize microtubules (green). Arrows show the disorganized mitotic spindles. DNA (blue) was stained DAPI. Scale bar, 20 μm.

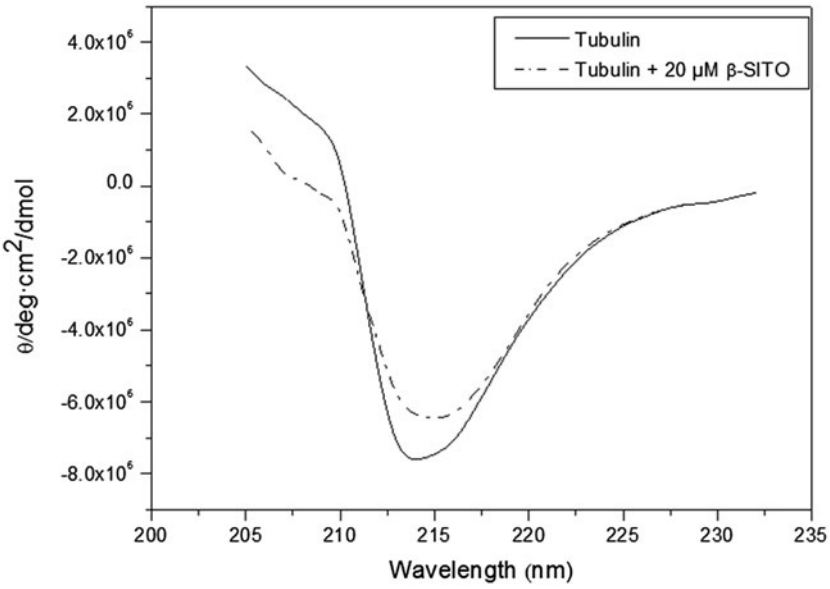

Figure 3. Far-UV circular dichroism spectra of tubulin in the absence (solid line), and presence of 20 μM β-SITO (dotted line). Tubulin (5 μM) was incubated without or with β-SITO for 45 min at 35 °C in 25 mM Pipes buffer and the CD spectra were obtained as described in Materials and Methods.

Table 1. Calculated binding free energy using MM-GBSA and MM-PBSA to ascertain the strength of interaction between β-SITO and β-tubulin isotypes. The energy components like van der Waals, electrostatic, polar solvation and non-polar solvation, contributing to the binding free energy were also estimated.

Contribution	αβ-I	αβ-II	αβ-III	αβ-IV	αβ-V	αβ-VI	αβ-VII	αβ-VIII
ΔE_{INT}	0	0	0	0	0	0	0	0
ΔE_{VDW}	−38.830	−57.946	−55.783	−45.084	−41.887	−63.242	−42.600	−52.298
ΔE_{ELE}	−14.795	−3.112	−3.946	.522	1.387	.001	−3.982	−8.304
$\Delta E_{GAS/\ \Delta E\ MM}$	−53.626	−61.058	−59.729	−44.562	−40.5	−63.241	−46.583	−60.602
ΔG_{PB}	30.148	26.952	25.230	27.958	17.686	36.196	27.692	28.625
$\Delta G_{SOL\text{-}NP}$	−3.792	−4.859	−4.907	−4.673	−3.856	−5.070	−3.864	−4.094
$\Delta G_{SOLV,PB}$	26.356	22.093	20.323	23.285	13.831	31.126	23.828	24.531
$\Delta G_{ELE,PB}$	11.561	18.981	16.377	23.807	15.218	31.127	19.845	16.227
$H_{TOT,PB}$	−27.270	−38.965	−39.406	−21.277	−26.669	−32.114	−22.755	−36.071
ΔG_{GB}	29.395	17.558	22.154	21.558	16.241	30.562	22.214	24.949
$\Delta G_{SOLV,GB}$	24.843	16.639	16.433	16.670	12.024	24.164	17.928	19.504
$\Delta G_{ELE\ GB}$	10.048	13.527	12.487	17.192	13.411	24.165	13.946	11.200
$H_{TOT,\ GB}$	−28.783	−44.419	−43.296	−27.892	−28.476	−42.792	−28.654	−41.097

by $\alpha\beta_{III}$ (−33.486 kcal/mol) in comparison to other isotypes. In order to refine the data, the docked complexes of β-SITO and β isotype-specific αβ-tubulin dimers were MD simulated for 25 ns (Figures 4 and 5). Figure 4 shows β-SITO's binding to specific β tubulin isotypes displayed as Time series of the root-mean-square deviations (RMSD) versus time. The equilibration of the MD trajectories was also monitored based on the convergence of plots of RMSD of Cα carbon atoms (Figure 4). The relative fluctuation in the RMSD of Cα carbon atoms (Cα-rmsd) was very small after 5 ns of simulation, representing convergence of the system. The overall RMSD ranges from 0 to 3.5 Å. Amino acids in all isotypes followed similar flexibility trend with some variations at the N- and C-terminal residues (Figure 5(A)). Secondary structures in all isotypes were also found to be well conserved (Figure 5(B)).

Next, we analyzed the binding affinities of β-SITO with each αβ-tubulin dimer using Molecular Mechanics Poisson–Boltzmann surface area (MM–PBSA) and its complementary, Molecular Mechanics with Generalized Born and Surface Area solvation (MM–GBSA) methods (Kollman et al., 2000). As shown in Table 1, β-SITO showed strongest binding with β_{III} isotype-specific αβ dimer ($H_{TOT,PB}$ = −39.406 kcal/mol) and β_{II} isotype-specific αβ dimer (−38.965 kcal/mol) followed by

Table 2. Identification of protein hot spot residues. All residues of αβ-tubulin dimer contributing more than −1 kcal/mol to the tubulin–β-SITO complex are listed in the table. The energy components like van der Waals, electrostatic, polar solvation and non-polar solvation, contributing to the binding free energy were also estimated.

Isotype	Residue	Van der waals	Non-polar solv.	Electrostatic	Polar solvation	Total
I	A:VAL73	−1.571	−.213	.659	−.037	−1.161
	B:LEU 41	−1.42	−.274	.176	−.02	−1.538
	B:PRO242	−1.397	−.186	.506	.01	−1.067
	B:GLN244	−2.107	−.327	1.034	−.01	−1.41
II	A:ALA179	−1.044	−.139	.073	.038	−1.072
	B:LEU245	−2.094	−.391	.168	.009	−2.308
	B:LEU252	−2.048	−.231	.444	−.081	−1.915
	B:ASN255	−1.324	−.12	.191	.157	−1.096
	B:MET256	−1.226	−.076	.382	−.494	−1.413
	B:THR311	−.964	−.041	−.144	−.08	−1.229
	B:VAL312	−1.244	−.045	.109	.077	−1.102
	B:ALA313	−1.324	−.174	.079	.009	−1.409
	B:LYS349	−2.245	−.197	.215	.114	−2.113
III	A:GLN175	−2.411	−.416	2.869	−1.648	−2.411
	A:VAL176	−2.573	−.322	−.063	.101	−2.857
	A:TYR223	−2.859	−.392	1.22	.023	−2.007
	B:LEU245	−1.493	−.172	.207	−.001	−1.458
	B:MET322	−1.872	−.396	.974	−.154	−1.448
	B:VAL325	−.969	−.06	−.203	.127	−1.104
	B:VAL350	−1.32	−.173	.254	.018	−1.221
IV	A:VAL176	−1.43	−.162	.471	−.076	−1.197
	A:ARG220	−2.426	−.392	1.305	.066	−1.446
	A:TYR223	−2.589	−.418	1.269	.033	−1.705
	B:LEU245	−1.329	−.183	.157	.021	−1.333
	B:VAL352	−1.804	−.296	.9	.007	−1.193
V	B:MET322	−2.474	−.454	.815	−.05	−2.163
	B:VAL325	−1.292	−.098	−.118	.064	−1.444
	B:VAL350	−1.804	−.296	.9	.007	−1.193
	B:VAL352	−2.565	−.396	.879	−.007	−2.089
VI	A:THR178	−1.617	−.094	.699	−.003	−1.015
	A:ALA179	−1.005	−.089	−.06	.007	−1.147
	B:LEU245	−2.892	−.297	.41	−.114	−2.892
	B:LYS251	−1.63	−.179	.71	.011	−1.088
	B:LEU252	−1.33	−.125	.24	−.122	−1.336
	B:LYS349	−1.394	−.183	.252	.267	−1.058
VII	A:TYR223	−2.899	−.254	.723	.135	−2.295
	B:GLN244	−2.097	−.384	1.128	−.027	−1.379
VIII	A:PRO174	−1.718	−.199	.397	−.161	−1.681
	A:GLN175	−2.396	−.232	1.047	.012	−1.569
	A:TYR223	−2.519	−.375	1.267	.004	−1.623
	B:MET322	−2.14	−.225	.869	−.073	−1.569
	B:VAL325	−.862	−.053	−.322	.193	−1.044
	B:THR350	−.857	−.142	1.276	−2.25	−1.973
	B:VAL352	−1.48	−.164	.081	−.013	−1.576

βv_{III}, β_{VI}, β_{I}, β_{V}, β_{VII} and β_{IV} specific αβ dimers based on MM-PBSA method. MM-GBSA method also yielded similar results (Table 1). The entropy contribution was not included explicitly in calculating relative free energy between related systems of isotypes which differ by only few amino acids, and assumed that solute entropy would be similar for all systems (Kumbhar, Borogaon, Panda, & Kunwar, 2016). Energy contribution of van der Waals (ΔE_{VDW}) and the electrostatic component (ΔE_{ELE}) were also estimated for all protein–ligand complexes. The van der Waals (ΔE_{VDW}) forces made significant contributions to the free energy of binding in all complexes (Table 1). The electrostatic component (ΔE_{ELE}), although favorable for some of the isotypes (β_{I}, β_{II}, β_{III}, β_{VI}, β_{VII}), the net polar contribution ($\Delta G_{(ele,PB/GB)} = \Delta E_{ele} + \Delta G_{(PB/GB)}$) for all β-SITO–β-tubulin isotype complexes was rendered unfavorable due to considerably large desolvation ($\Delta G_{PB/GB}$) penalty. However, the net non-polar components ΔE_{vdw} and $\Delta G_{sol\text{-}np}$ were observed to make highly favorable contribution to the binding free energy (Figure 6).

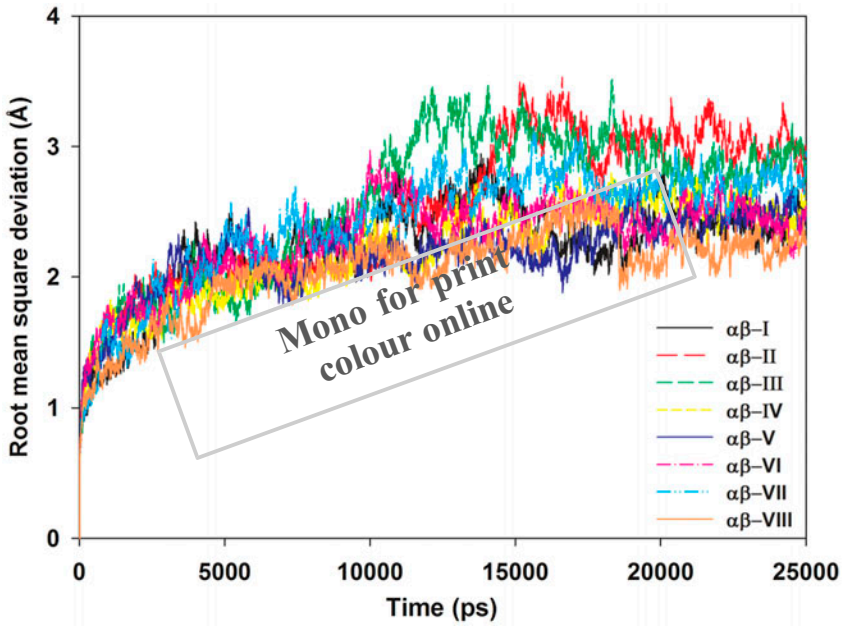

Figure 4. Molecular dynamic simulations of β-SITO binding to specific β tubulin isotypes displayed as time series of the RMSD over 25 ns.

Energy contribution of every amino acid of β isotypes specific αβ-tubulin dimers for β-SITO–binding was also calculated using the MM-GBSA method, implemented in Amber 11. Those residues that contributed more than −1.0 kcal/mol to the stability of the complexes were identified as hot spot amino acids (Table 2). Two or more hot spots were identified for each complex (Table 2). It must also be noted that the residues which were found to have an energy contribution of more than −1 kcal/mol are therefore important for the binding of β-SITO with the isotype specific β-tubulin in αβ dimers. Most of these hot-spot amino acids interacted with the compound through both hydrogen bonding and hydrophobic interactions (Figure 7). The three-dimensional representation of the binding of β-SITO with tubulin isotypes (β_I–β_{VIII}) are shown in Figure 8.

Discussion

Identification of molecules that possess cancer preventive properties as well as chemotherapeutic potential holds huge promise in the fight against cancer. Several natural products – both from the sea and from land – have been known to possess these qualities (Fedorov, Ermakova, Zvyagintseva, & Stonik, 2013; Jin, Quan, Hou, & Fan, 2016; Khazir, Riley, Pilcher, De-Maayer, & Mir, 2014; Lopus, 2013; Lopus & Naik, 2015). Phytosterols, present in abundance in a wide variety of edible vegetables, are known for their ability to prevent development of certain types of cancers and for their chemotherapeutic potential with minimal or no side effects (Ovesna, Vachalkova, & Horvathova, 2004; Woyengo, Ramprasath, & Jones, 2009). In this study, we chose to examine the chemotherapeutic potential of one such phytosterol, β-SITO, and elucidated its β-tubulin isotype-specific binding interactions using computational docking and atomistic MD simulations.

β-SITO inhibits MCF-7 cell viability and migration

First, we examined the effect of β-SITO on the proliferative potential of MCF-7 breast tumor cells. The phytosterol inhibited the cell viability with an IC_{50} of 10 ± 1 μM (Figure 1(B)). While investigating its anti-invasive efficacy, it was found that β-SITO strongly inhibits MCF-7 cell migration, as evidenced by an *in vitro* wound-healing assay (Figure 1(C)), indicating its potential as an antimetastatic agent. Invasion and metastasis of cancer from its primary location to different parts of the body pose a great challenge in effective clinical management of many tumor types. Cancer metastasis involves detachment of the cells from its original location and their subsequent migration to different parts of the body – either through blood stream or through lymphatic circulation. Drugs that can prevent cancer cell migration therefore hold huge therapeutic potential (Field, Kanakkanthara, & Miller, 2014; Yang, Ganguly, & Cabral, 2010). Since β-SITO is a tubulin binding agent (Mahaddalkar et al., 2015), we examined its effect on cellular microtubules using immunofluorescence staining

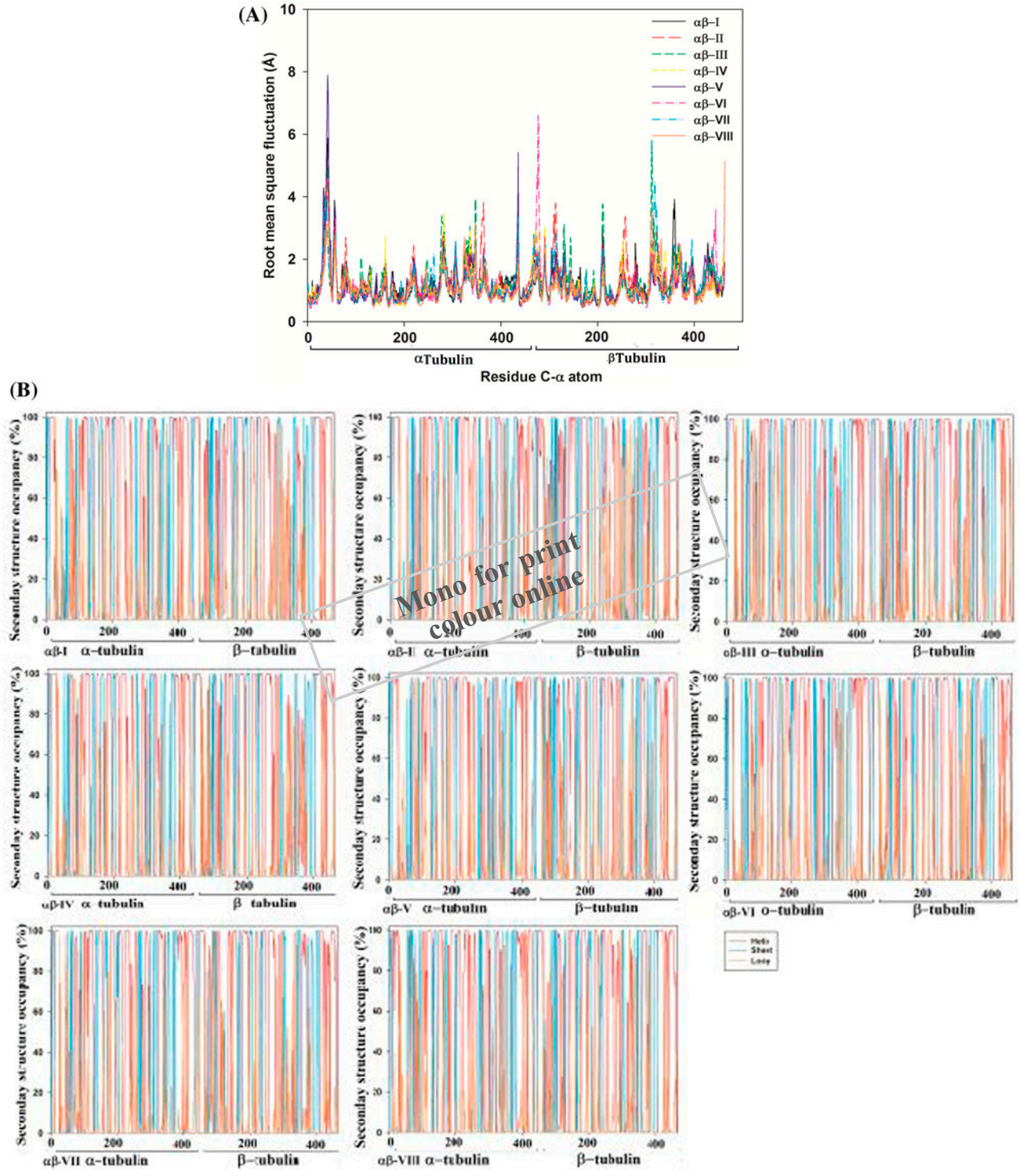

Figure 5. (A) Root mean square fluctuation of each residue calculated over 25 ns of MD simulation for β-SITO bound to specific β tubulin isotypes. (B) Secondary structure occupancy for all β-SITO bound to specific β tubulin isotypes calculated calculate over 25 ns of MD simulation.

in the drug-treated cells. The microtubules showed disruption of microtubules and disorganization of mitotic chromosomes, suggesting that the compound inhibits cancer cell viability at least in part by targeting cellular microtubules and disrupting their structural integrity (Figure 2).

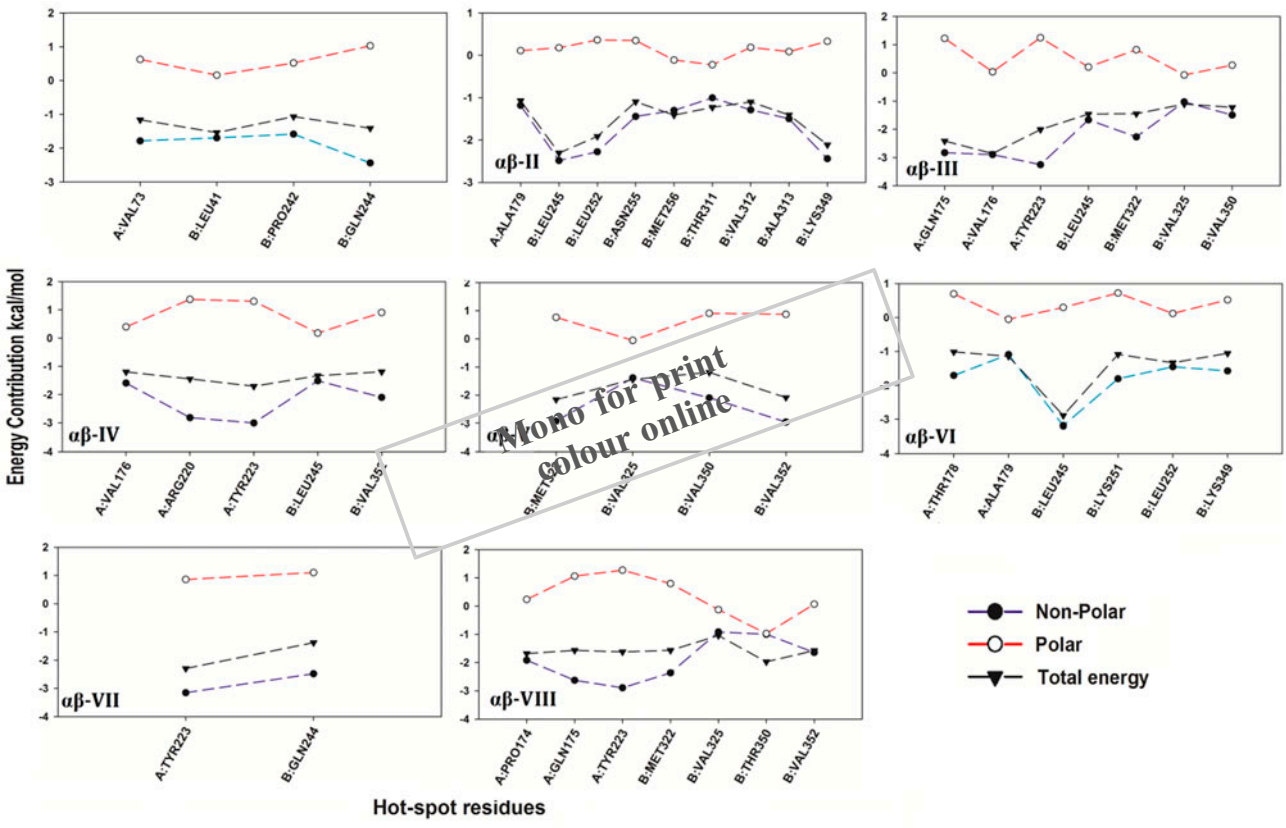

Figure 6. Hotspot amino acids and their energy contributions in β-SITO-β-tubulin isotype binding. Energy contributions of each amino acid for the binding interactions over last 500 frames were calculated using MM-PBSA and MM-GBSA methods.

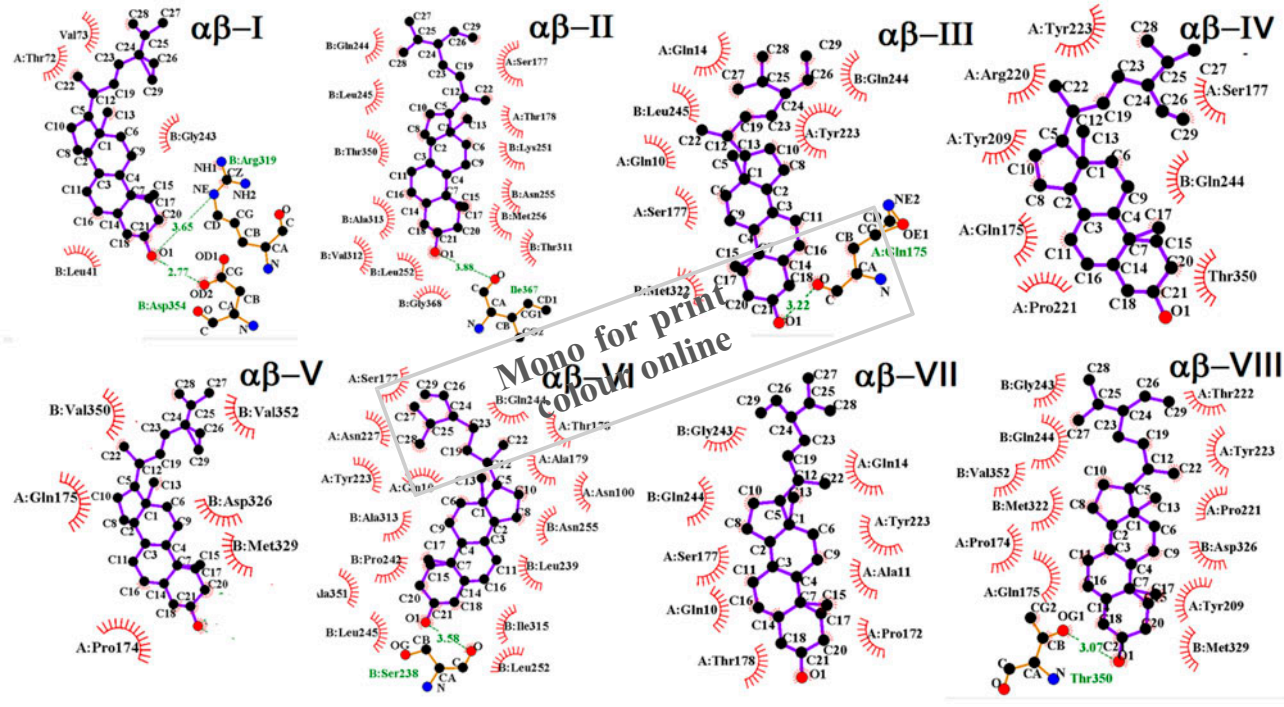

Figure 7. 2-D representation of interactions between β-sitosterol and tubulin isotypes, calculated after Molecular dynamics simulation. Ligplot shows the amino acids involved in hydrogen bond formation and hydrophobic interaction.

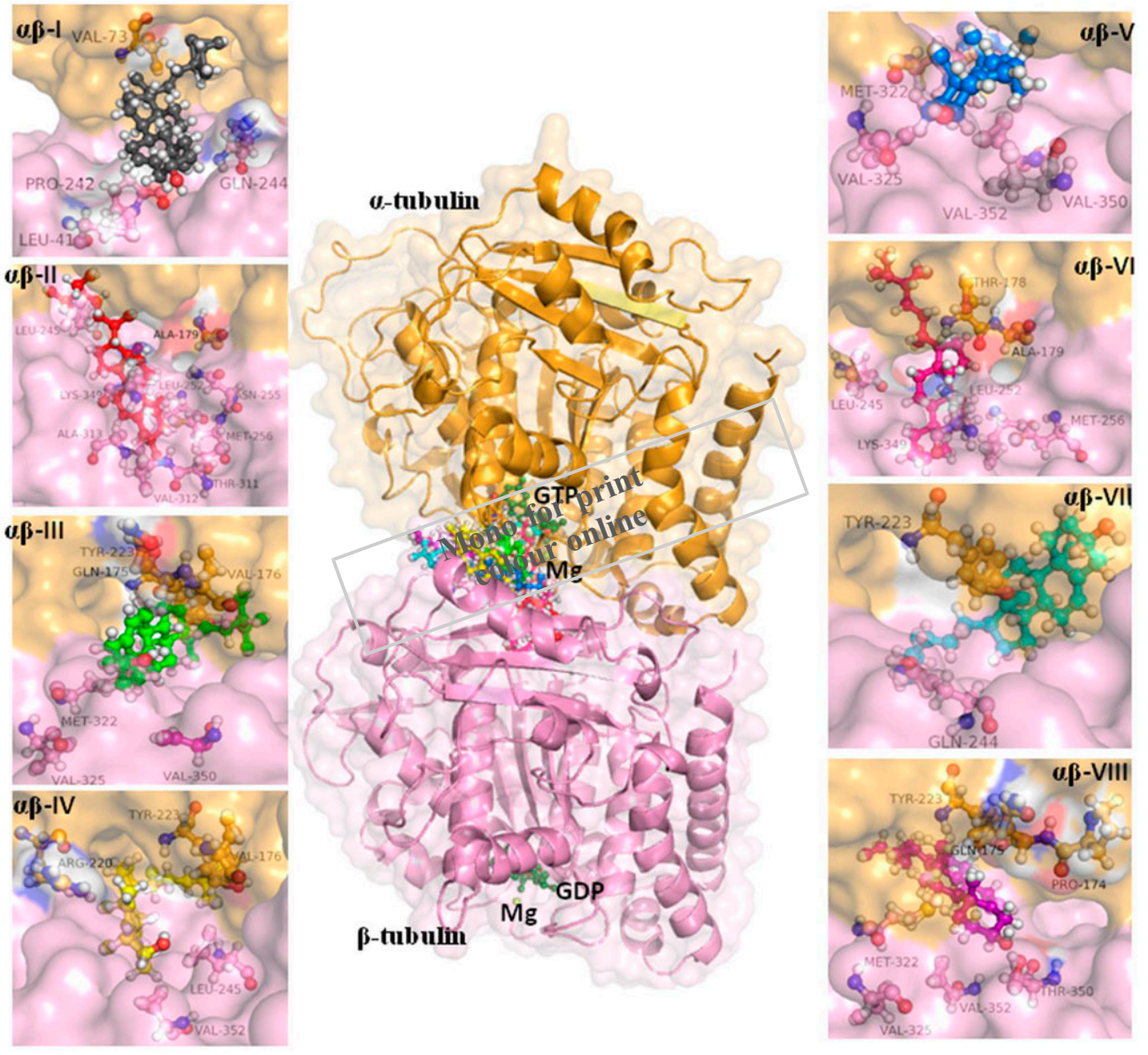

Figure 8. Three-dimensional representation of the binding of β-SITO with tubulin isotypes (β_I–β_{VIII}). The center image shows that β-SITO lodges itself in similar binding pockets in all eight β-tubulin isotypes. β-SITO binds to β_{II} (red) and β_{VI} (magenta) in a manner similar to each other but distinct with other isoforms. The figure also illustrates the spatial arrangement of the hot spot amino acids around the ligand. Mg is represented as yellow sphere while GDP and GTP in olive green ball and stick model.

β-SITO altered the secondary conformation of tubulin

Far-UV circular dichroism has been routinely used for identification of conformational changes of proteins whose secondary structure would alter when bound to a targeted ligand (de Pereda, Leynadier, Evangelio, Chacón, & Andreu, 1996). Using purified tubulin, we identified that β-SITO is capable of altering the secondary structure of tubulin as evidenced by a reduction in the negative band, compared to the control (Figure 3). To our knowledge, it is the first evidence of the phytosterol's ability to disrupt the secondary structural integrity of tubulin, and suggest that the loss of helical integrity of tubulin (Figure 3) played a role in the drug-induced disruption of cellular microtubules (Figure 2).

Molecular characterization of β-SITO binding to tubulin isotypes

Alterations near the C-terminus of β-tubulin result in the formation of multiple tubulin 'isotypes' (Janke, 2014). Although their functions are poorly understood, they have been known to show tissue-specific expression.

For example, whereas β_I and β_V isotype are expressed in almost all tissues, β_{II} and β_{III} are expressed mainly in brain. β_{VI} has been reported to be expressed in hematopoietic tissues (Burgoyne, Cambray-Deakin, Lewis, Sarkar, & Cowan, 1988; Sullivan & Cleveland, 1986). We investigated the relative binding affinities of β-SITO with all known isotypes of β-tubulin using computational docking, molecular dynamic simulations, and MM-PBSA and MM-GBSA calculations (Figures 4–8 and Supplementary Figure S2). We found that the phytosterol shows highest affinity to β_{II} and β_{III} isotypes (Table 1). It may also be noted that β-SITO binds to β_{III} in a manner that is distinct with other isoforms (Figure 7). On a clinical point of view, overexpression of β_{II} and β_{III} isotypes has been associated with drug resistance against antitubulin drugs (Dumontet & Jordan, 2010; Lebok et al., 2016; Lopus et al., 2015; Shalli, Brown, Heys, & Schofield, 2005; Wilson et al., 2015). For instance, β_{II}-tubulin has been associated with paclitaxel-resistant ovarian cancer cell lines and docetaxel-resistant breast cancer cells (Kavallaris et al., 1997; Shalli et al., 2005). Kanakathara et al., demonstrated that silencing of β_{II}-tubulin and β_{III}-tubulin can sensitize ovarian cancer cells to peloruside A and laulimalide (Kanakkanthara, Northcote, & Miller, 2012). Specific silencing of β_{II}-tubulin was reported to sensitize lung cancer cells to vinca alkaloids (Gan & Kavallaris, 2008). Although the mechanisms of β_{II}-tubulin-associated resistance are poorly understood, the ability of β_{II}-tubulin to resist taxol-mediated suppression of microtubule dynamic instability (Derry, Wilson, Khan, Ludueña, & Jordan, 1997) might be a contributing factor in this regard. By its high-affinity binding to β_{III} and β_{II}-tubulin, β-SITO demonstrated its therapeutic potential against drug resistance associated with these tubulin isotypes. In summary, we found β-SITO as a potential tubulin-targeted anticancer agent that specifically targets β_{II} and β_{III} tubulin isotypes that have been implicated in anticancer drug resistance.

Acknowledgements

The authors thank UM-DAE CBS (MP and ML) for financial support. We thank Prof. Dulal Panda, Indian Institute of Technology Bombay, for the use of Nikon eclipse TE1000-U microscope. We thank Dr. Sanith C and Ms. Tejashree Mahaddalkar for critical reading of the manuscript.

Disclosure statement

No potential conflict of interest was reported by the authors.

Funding

This work was supported by the UM-DAE Centre for Excellence in Basic Sciences [grant number 1].

Supplementary material

The supplementary material for this paper is available online at http://dx.doi.org.10.1080/07391102.2016.1271749.

References

Allnér, O., Nilsson, L., & Villa, A. (2012). Magnesium ion–water coordination and exchange in biomolecular simulations. *Journal of Chemical Theory and Computation, 8*, 1493–1502.

Awad, A. B., Chen, Y. C., Fink, C. S., & Hennessey, T. (1996). beta-Sitosterol inhibits HT-29 human colon cancer cell growth and alters membrane lipids. *Anticancer Research, 16*, 2797–2804.

Awad, A. B., Downie, A., Fink, C. S., & Kim, U. (2000). Dietary phytosterol inhibits the growth and metastasis of MDA-MB-231 human breast cancer cells grown in SCID mice. *Anticancer Research, 20*, 821–824.

Awad, A. B., & Fink, C. S. (2000). Phytosterols as anticancer dietary components: Evidence and mechanism of action. *Journal of Nutrition, 130*, 2127–2130.

Becke, A. D. (1993). A new mixing of Hartree-Fock and local density-functional theories. *The Journal of Chemical Physics, 98*, 1372–1377.

Berendsen, H. J., Postma, J. V., van Gunsteren, W. F., DiNola, A., & Haak, J. (1984). Molecular dynamics with coupling to an external bath. *The Journal of Chemical Physics, 81*, 3684–3690.

Binkley, J. S., Pople, J. A., & Hehre, W. J. (1980). Self-consistent molecular orbital methods. 21. Small split-valence basis sets for first-row elements. *Journal of the American Chemical Society, 102*, 939–947.

Burgoyne, R. D., Cambray-Deakin, M. A., Lewis, S. A., Sarkar, S., & Cowan, N. J. (1988). Differential distribution of beta-tubulin isotypes in cerebellum. *EMBO Journal, 7*, 2311–2319.

Case, D. A., Cheatham, T. E., 3rd, Darden, T., Gohlke, H., Luo, R., Merz, K. M., Jr., … Woods, R. J. (2005). The Amber biomolecular simulation programs. *Journal of Computational Chemistry, 26*, 1668–1688. doi:10.1002/jcc.20290

Case, D. A., Darden, T. A., Cheatham, T. E., III, Simmerling, C. L., Wang, J., Duke, R. E., … Kollman, P. A. (2010). *AMBER 11*. San Francisco, CA: University of California.

Darden, T., York, D., & Pedersen, L. (1993). Particle mesh Ewald: An N·log(N) method for Ewald sums in large systems. *The Journal of Chemical Physics, 98*, 10089–10092.

Dave, R. H., Saengsawang, W., Lopus, M., Dave, S., Wilson, L., & Rasenick, M. M. (2011). A molecular and structural mechanism for g protein-mediated microtubule destabilization. *Journal of Biological Chemistry, 286*, 4319–4328.

de Pereda, J. M., Leynadier, D., Evangelio, J. A., Chacón, P., & Andreu, J. M. (1996). Tubulin secondary structure analysis, limited proteolysis sites, and homology to FtsZ. *Biochemistry, 35*, 14203–14215. doi:10.1021/bi961357b

Derry, W. B., Wilson, L., Khan, I. A., Ludueña, R. F., & Jordan, M. A. (1997). Taxol differentially modulates the dynamics of microtubules assembled from unfractionated and purified β-Tubulin Isotypes †. *Biochemistry, 36*, 3554–3562. doi:10.1021/bi962724m

Dumontet, C., & Jordan, M. A. (2010). Microtubule-binding agents: A dynamic field of cancer therapeutics. *Nature Reviews Drug Discovery, 9*, 790–803. doi:10.1038/nrd3253

Essmann, U., Perera, L., Berkowitz, M. L., Darden, T., Lee, H., & Pedersen, L. G. (1995). A smooth particle mesh Ewald method. *The Journal of Chemical Physics, 103*, 8577–8593. doi:10.1021/acs.jctc.5b00190

Fedorov, S. N., Ermakova, S. P., Zvyagintseva, T. N., & Stonik, V. A. (2013). Anticancer and cancer preventive properties of marine polysaccharides: Some results and prospects. *Marine Drugs, 11*, 4876–4901. doi:10.3390/md11124876

Field, J. J., Kanakkanthara, A., & Miller, J. H. (2014). Microtubule-targeting agents are clinically successful due to both mitotic and interphase impairment of microtubule function. *Bioorganic & Medicinal Chemistry, 22*, 5050–5059. doi:10.1016/j.bmc.2014.02.035

Gan, P. P., & Kavallaris, M. (2008). Tubulin-targeted drug action: Functional significance of class ii and class IVb beta-tubulin in vinca alkaloid sensitivity. *Cancer Research, 68*, 9817–9824. doi:10.1158/0008-5472.CAN-08-1501

Janke, C. (2014). The tubulin code: Molecular components, readout mechanisms, and functions. *The Journal of Cell Biology, 206*, 461–472. doi:10.1083/jcb.201406055

Jiménez-Escrig, A., Santos-Hidalgo, A. B., & Saura-Calixto, F. (2006). Common sources and estimated intake of plant sterols in the Spanish diet. *Journal of Agricultural and Food Chemistry, 54*, 3462–3471. doi:10.1021/jf053188k

Jin, L., Quan, C., Hou, X., & Fan, S. (2016). Potential pharmacological resources: Natural bioactive compounds from marine-derived fungi. *Marine Drugs, 14*, 76. doi:10.3390/md14040076

Jorgensen, W. L., Chandrasekhar, J., Madura, J. D., Impey, R. W., & Klein, M. L. (1983). Comparison of simple potential functions for simulating liquid water. *The Journal of Chemical Physics, 79*, 926–935.

Kanakkanthara, A., Northcote, P. T., & Miller, J. H. (2012). betaII-tubulin and betaIII-tubulin mediate sensitivity to peloruside A and laulimalide, but not paclitaxel or vinblastine, in human ovarian carcinoma cells. *Molecular Cancer Therapeutics, 11*, 393–404. doi:10.1158/1535-7163.MCT-11-0614

Kavallaris, M., Kuo, D. Y., Burkhart, C. A., Regl, D. L., Norris, M. D., Haber, M., & Horwitz, S. B. (1997). Taxol-resistant epithelial ovarian tumors are associated with altered expression of specific beta-tubulin isotypes. *Journal of Clinical Investigation, 100*, 1282–1293. doi:10.1172/JCI119642

Khazir, J., Riley, D. L., Pilcher, L. A., De-Maayer, P., & Mir, B. A. (2014). Anticancer agents from diverse natural sources. *Natural Product Communications, 9*, 1655–1669.

Kollman, P. A., Massova, I., Reyes, C., Kuhn, B., Huo, S., Chong, L., … Wang, W. (2000). Calculating structures and free energies of complex molecules: combining molecular mechanics and continuum models. *Accounts of Chemical Research, 33*, 889–897.

Kumbhar, B. V., Borogaon, A., Panda, D., & Kunwar, A. (2016). Exploring the origin of differential binding affinities of human tubulin isotypes αβII, αβIII and αβIV for DAMA-colchicine using homology modelling, molecular docking and molecular dynamics simulations. *PLoS ONE, 11*, e0156048.

Lebok, P., Ozturk, M., Heilenkotter, U., Jaenicke, F., Muller, V., Paluchowski, P., … Quaas, A. (2016). High levels of class III β-tubulin expression are associated with aggressive tumor features in breast cancer. *Oncology Letters, 11*, 1987–1994.

Lopus, M. (2013). Mechanism of mitotic arrest induced by dolastatin 15 involves loss of tension across kinetochore pairs. *Molecular and Cellular Biochemistry, 382*, 93–102.

Lopus, M., Manatschal, C., Buey, R. M., Bjelić, S., Miller, H. P., Steinmetz, M. O., & Wilson, L. (2012). Cooperative stabilization of microtubule dynamics by EB1 and CLIP-170 involves displacement of stably bound P(i) at microtubule ends. *Biochemistry, 51*, 3021–3030.

Lopus, M., & Naik, P. K. (2015). Taking aim at a dynamic target: Noscapinoids as microtubule-targeted cancer therapeutics. *Pharmacological Reports, 67*, 56–62.

Lopus, M., Smiyun, G., Miller, H., Oroudjev, E., Wilson, L., & Jordan, M. A. (2015). Mechanism of action of ixabepilone and its interactions with the βIII-tubulin isotype. *Cancer Chemotherapy and Pharmacology, 76*, 1013–1024. doi:10.1007/s00280-015-2863-z

Mahaddalkar, T., Naik, P. K., Choudhary, S., Manchukonda, N., Kantevari, S., & Lopus, M. (2016). Structural investigations into the binding mode of a novel noscapine analogue, 9-(4-vinylphenyl) noscapine, with tubulin by biochemical analyses and molecular dynamic simulations. *Journal of Biomolecular Structure and Dynamics, 31*, 1–10.

Mahaddalkar, T., Suri, C., Naik, P. K., & Lopus, M. (2015). Biochemical characterization and molecular dynamic simulation of β-sitosterol as a tubulin-binding anticancer agent. *European Journal of Pharmacology, 760*, 154–162. doi:10.1016/j.ejphar.2015.04.014

Massova, I., & Kollman, P. A. (2000). Combined molecular mechanical and continuum solvent approach (MM-PBSA/GBSA) to predict ligand binding. *Perspectives in Drug Discovery and Design, 18*, 113–135.

Meagher, K. L., Redman, L. T., & Carlson, H. A. (2003). Development of polyphosphate parameters for use with the AMBER force field. *Journal of Computational Chemistry, 24*, 1016–1025.

Ovesna, Z., Vachalkova, A., & Horvathova, K. (2004). Taraxasterol and beta-sitosterol: New naturally compounds with chemoprotective/chemopreventive effects. *Neoplasma, 51*, 407–414.

Pearlman, D. A., Case, D. A., Caldwell, J. W., Ross, W. S., Cheatham, T. E., DeBolt, S., … Kollman, P. (1995). AMBER, a package of computer programs for applying molecular mechanics, normal mode analysis, molecular dynamics and free energy calculations to simulate the structural and energetic properties of molecules. *Computer Physics Communications, 91*, 1–41.

Santoshi, S., & Naik, P. K. (2014). Molecular insight of isotypes specific β-tubulin interaction of tubulin heterodimer with noscapinoids. *Journal of Computer-Aided Molecular Design, 28*, 751–763. doi:10.1007/s10822-014-9756-9

Shalli, K., Brown, I., Heys, S. D., & Schofield, A. C. (2005). Alterations of beta-tubulin isotypes in breast cancer cells resistant to docetaxel. *FASEB Journal, 19*, 1299–1301. doi; 10.1096/fj.04-3178fje

Sitkoff, D., Sharp, K. A., & Honig, B. (1994). Accurate calculation of hydration free energies using macroscopic solvent models. *The Journal of Physical Chemistry, 98*, 1978–1988.

Sullivan, K. F., & Cleveland, D. W. (1986). Identification of conserved isotype-defining variable region sequences for four vertebrate beta tubulin polypeptide classes. *Proceedings of the National Academy of Sciences, 83*, 4327–4331.

von Holtz, R. L., Fink, C. S., & Awad, A. B. (1998). β-sitosterol activates the sphingomyelin cycle and induces apoptosis in LNCaP human prostate cancer cells. *Nutrition and Cancer, 32*, 8–12. doi:10.1080/01635589809514709

Vundru, S. S., Kale, R. K., & Singh, R. P. (2013). beta-Sitosterol induces G1 arrest and causes depolarization of mitochondrial membrane potential in breast carcinoma MDA-MB-231 cells. *BMC Complementary and Alternative Medicine, 13*, 1472–6882. doi:10.1186/1472-6882-13-280

Wilson, L., Lopus, M., Miller, H. P., Azarenko, O., Riffle, S., Smith, J. A., & Jordan, M. A. (2015). Effects of eribulin on microtubule binding and dynamic instability are strengthened in the absence of the βIII tubulin isotype. *Biochemistry, 54*, 6482–6489. doi:10.1021/acs.biochem.5b00745

Woyengo, T. A., Ramprasath, V. R., & Jones, P. J. (2009). Anticancer effects of phytosterols. *European Journal of Clinical Nutrition, 63*, 813–820. doi:10.1038/ejcn.2009.29

Yang, H., Ganguly, A., & Cabral, F. (2010). Inhibition of cell migration and cell division correlates with distinct effects of microtubule inhibiting drugs. *Journal of Biological Chemistry, 285*, 32242–32250. doi:10.1074/jbc.M110.160820